

Estimation of a Color Uniformity Index in Mandarins Using an Artificial Intelligence-Based System

1st Kevin Bautista*

*Department of electrical, electronics
and telecommunications engineering
Universidad Industrial de Santander
Bucaramanga, Santander
kevin2201143@correo.uis.edu.co*

2nd Joseph Trigos Delgado*

*Department of electrical, electronics
and telecommunications engineering
Universidad Industrial de Santander
Bucaramanga, Santander
joseph2201832@correo.uis.edu.co*

3rd Sergio Urrea

*Department of electrical, electronics
and telecommunications engineering
Universidad Industrial de Santander
Bucaramanga, Santander
sergio2228328@correo.uis.edu.co*

4th Henry Arguello

*Department of Systems Engineering
Universidad Industrial de Santander
Bucaramanga, Santander
henarfuf@uis.edu.co*

5th Hans Garcia

*Department of electrical, electronics
and telecommunications engineering
Universidad Industrial de Santander
Bucaramanga, Santander
hayegaar@uis.edu.co*

Abstract—In the agricultural industry, color uniformity is currently considered a key criterion for determining fruit quality and commercial acceptability, especially in citrus, where color uniformity is particularly relevant, as it is closely related to the degree of ripeness, perceived freshness and overall product attractiveness. Among citrus fruits such as lemon, mandarin, grapefruit, orange, mandarin stands out as an important crop due to its high demand and consumer sensitivity to color variations, which makes uniformity in appearance directly influence buyer perception and compliance with trade standards. However, the evaluation of color uniformity is still done manually, which introduces subjectivity, errors and inconsistency in grading processes, negatively impacting the efficiency and competitiveness of producers. Several studies have explored the analysis of citrus using artificial intelligence. However, many of these efforts face limitations related to image quality, lack of standardization in capture conditions, or limited adaptation to local contexts such as the Colombian market. To address these challenges, an artificial intelligence-based system was developed to quantitatively assess color uniformity in postharvest mandarins. The system incorporates an image acquisition subsystem, followed by detection, segmentation and data analysis procedures to calculate a color uniformity index, with the objective of improving the selection and classification processes in the citrus industry within the Colombian sector. The use of an artificial intelligence algorithm and the definition of a quantitative index of color uniformity in mandarin oranges is proposed in order to provide agricultural producers with an objective and accurate tool to optimize the classification of their fruits.

Index Terms—Uniformity , color, mandarin, index.

I. INTRODUCTION

In Colombia, agriculture is a key activity for the country's economic and social development, as it contributes to food

security and supports multiple production chains [1]. Its importance in the production of citrus fruits—such as oranges, tangerines, lemons, grapefruits, and other varieties native to Colombia's biodiversity—plays a crucial role in the economic development of producing regions. According to data reported by the Ministry of Agriculture and Rural Development in 2021 [2], the northeastern and western regions of the country, which account for 57% of citrus harvests, have approximately 50,000 hectares dedicated to their cultivation.

An important parameter that influences the perceived quality of fruit and its commercial acceptance by consumers is color uniformity, as it serves as a visual indicator of freshness, ripeness, and flavor. Uniformity is also associated with product quality [3]. Therefore, ensuring a uniform color helps maintain the product's commercial value, satisfies market expectations, and sustains competitiveness within the agricultural industry.

Currently, color uniformity is assessed through conventional methods—namely, manual procedures based on human visual evaluation to determine quality based on general appearance—which makes the process prone to errors [4]. Due to the low efficiency of manual classification, the commercialization process of the product slows down, potentially leading to serious economic consequences for farmers. Product quality may also be compromised, reducing access to important citrus markets.

The lack of an automated and standardized system in Colombia to quantitatively characterize color uniformity in mandarins represents a major challenge for the country's agricultural industry, especially considering that mandarins play a fundamental role in the economy of several producing regions, including Simacota, Santander, where Israeli mandarins are

* Both authors contributed equally to this work.

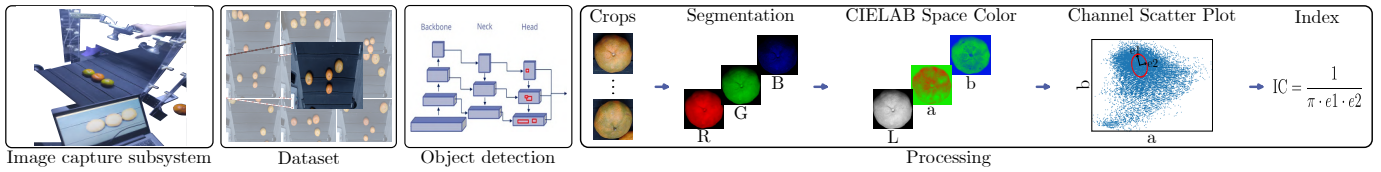


Fig. 1. Proposed system method for color uniformity estimation in mandarin oranges. A subsystem for image capture is designed, a data set is created, an algorithm for object detection is applied and finally, data processing is performed.

grown. For this reason, manual evaluation continues to be a method that reduces competitiveness among producers and limits access to markets that demand products with homogeneous characteristics.

Our work consisted of the design and implementation of a system capable of quantifying color uniformity in post-harvest mandarins, using artificial intelligence techniques such as computer vision. The project began with the implementation of an image capture system composed of a digital camera, a conveyor belt and a lighting environment. Subsequently, a data set was created to train YOLO-based algorithm to detect mandarins in the images. As a last step, the data were processed, arriving at the definition of the color uniformity index in mandarins.

II. RELATED WORKS

Color is one of the main attributes evaluated in agricultural products, as consumers naturally associate color with the ripeness or quality of the product [5]. In the case of mandarins, color is a decisive factor in the selection process; during harvest, they are picked manually and then sorted into containers according to the uniformity of their color [6].

In the industry, colorimeters such as the PCE-CSM 1 [7] are commonly used. The device is an electronic instrument specialized in color measurement, allowing quality control to be carried out with high precision according to the selected color space. Another tool used in the industry for color measurement consists of a set of cards developed by the Postharvest Department of the Valencian Institute of Agricultural Research (IVIA) [5]. These cards emulate color shades for oranges and mandarins based on the index

$$CI = \frac{1000 \cdot a}{L \cdot b}, \quad (1)$$

where a and b are scalars that give value to the chromatic components, and L is also a scalar that represents the luminance component for a specific color in the CIELAB.

One of the main limitations of traditional colorimeters, such as the PCE-CSM 1, is their small measurement area, which prevents obtaining representative values in fruits with non-uniform coloration. Additionally, the high cost of these devices limits their adoption by small and medium-sized producers. For this reason, a system based on artificial intelligence that enables the analysis of the surface of the fruit and the calculation of a quantitative color uniformity index represents a more accurate and accessible solution for classification processes in the agricultural industry.

III. COLOR UNIFORMITY ESTIMATION SYSTEM

To estimate the color uniformity in mandarins, a system was designed comprising modules that enable the efficient capture, processing, and analysis of information obtained from the mandarins. The proposed system includes an image acquisition subsystem, a mandarin detection algorithm, image processing techniques, a color space, and a statistical analysis used to define the uniformity index.

A. Image capture subsystem

A Logitech camera was positioned 43 cm above the conveyor belt to capture clear images of multiple mandarins simultaneously, ensuring data consistency. The camera resolution was set to 1920×1080 pixels, providing an optimal balance between image quality and processing efficiency. Lower resolutions would compromise color analysis, while higher resolutions would unnecessarily increase file size. Additionally, an integration time of 15.6 ms was configured, allowing for adequate light capture without compromising image sharpness.

A conveyor belt system from the optics lab was used to capture moving images of mandarin oranges. It consists of a NEMA 17 stepper motor, a TB6600 controller and a Raspberry Pi Pico microcontroller. The motor converts digital signals into precise motions, allowing accurate control of the belt motion. The TB6600 controller manages the operation of the motor allowing the current to be adjusted between 0.5 A and 3.5 A, as well as setting the steps per revolution as required. The Raspberry Pi Pico acts as the central processing unit, responsible for setting the motor parameters and running the control software, developed in MicroPython for its ease of use and suitability for embedded systems. Most of the devices that make up the image capture subsystem are shown in figure 1.

To select the lighting subsystem, tests were conducted with three light configurations, starting with two pairs of LED strips positioned perpendicular to the conveyor belt, followed by two incandescent bulbs directed towards the capture area, and finally, a pair of LED tubes accompanied by a diffuser sheet installed at the top of the laboratory, located approximately 2 meters above the image capture area. Each of these configurations was evaluated in terms of color perception and reflection on the mandarins, considering the uniformity and consistency necessary for image capture. In addition to the perceptual evaluation, a theoretical analysis was performed using an

Ocean Insight flame vis-nir spectrometer alongside OceanView software to examine the spectral behavior of each light source within the 500 to 630 nm range, which encompasses the green and red colors that characterize the ripening process of mandarins. Figure 2 presents the spectra obtained, from which it can be deduced that the LED tube pair provided the optimum illumination for the application, as it falls within the required range and presented the greatest uniformity in intensity values among the three options considered.

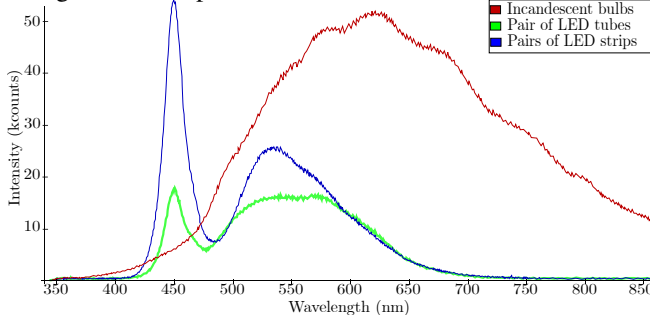


Fig. 2. Spectra resulting from the three lighting options considered.

B. Algorithm for the detection of mandarin

For the proposed method, the analysis of color change in mandarins required the use of high-resolution images to capture these color changes in detail. In consideration of the high pixel content, performing individual or group pixel analysis increases training time and demands a large processing power on the GPU of a laptop with limited resources [8]. For these reasons, YOLO-based algorithm is used, which with one stage allows to detect objects, reducing considerably the training time. A comparison was made between 17 different YOLO architectures, considering the 4 most recent versions (YOLOv8 to YOLOv11) and their respective subversions in which the number of trainable parameters varies. For the training of each architecture, use was made of the capture subsystem, generating a total of 270 images that were subsequently labeled at 255 [9]. The selection was based on two objective criteria: the mAP50-95 value obtained with the validation set and the number of trainable parameters of the architecture. Figure 3 shows the validation performance of the 17 architectures.

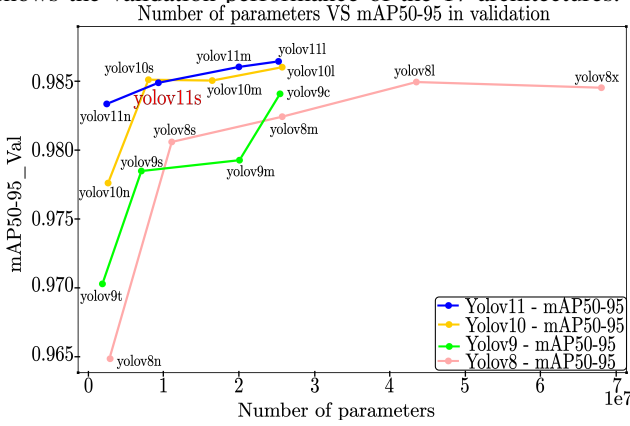


Fig. 3. Performance graph of different YOLO versions based on the number of trainable parameters and the mAP50-95 performance metric.

C. Images Processing

As a result of the training of the YOLOv11s model, we obtained the mandarin clipping (YOLO calls them 'crops') present in the test images with a value of 0.985 in the performance metric mAP50-95, the *crops* include information of the mandarin and the conveyor belt. In order to store only the pixels of the mandarin *crops*, the segmentation of the mandarin was performed to facilitate the analysis in the measurement of its chromatic uniformity. Once the region of interest was obtained, we proceeded to improve the isolation by calculating a matrix of ratios between the red channel and the blue channel of the pixels

$$\mathbf{F}_{x,y} = \frac{\mathbf{R}_{x,y}}{\mathbf{B}_{x,y}}, \quad (2)$$

eliminating much of the background and leaving the tangerine pixels ready for color analysis. $\mathbf{F}_{x,y}$ represents the ratio matrix, $\mathbf{R}_{x,y}$ corresponds to the red channel of the image and $\mathbf{B}_{x,y}$ to the blue channel, all defined in terms of the spatial coordinates (x, y).

Once the ratio matrix is obtained, a binary mask is created by applying a threshold to the red-blue ratio matrix. Values greater than 0.95 are marked as True, while values less than the threshold are marked as False. The threshold of 0.95 was determined by analyzing the histogram of the red-blue ratio in multiple images of mandarins. In Figure 4-a and Figure 4-b, an example of the original image and the corresponding histogram of the red-over-blue division are shown, respectively. Finally, the obtained mask is applied to the original image, yielding the segmented mandarin as illustrated in Figure 4-c.

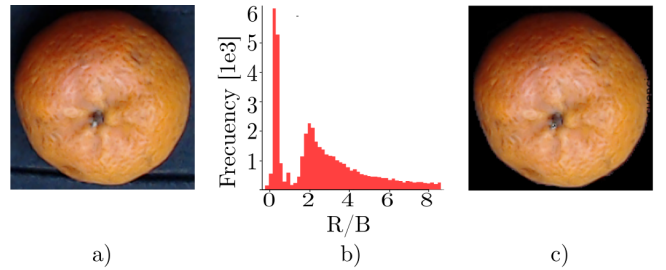


Fig. 4. a) Original mandarin after passing through YOLO. b) Histogram of the ratio matrix between the red and blue channels of the mandarin image. c) Segmented mandarin after masking.

D. Color space for index definition

To objectively analyze the color of mandarins, it is essential to understand the different color spaces and the purposes for which they were developed. The RGB color space is involved in the image acquisition process for our work; however, its primary goal is to represent colors according to the sensitivity of the sensors in the device. This implies that identical RGB intensity values can be perceived differently depending on sensor sensitivity. The RGB color space's dependency on the sensor introduces inaccuracy in the objective assessment of color uniformity in mandarins.

The CIELAB color space, on the other hand, is designed to closely emulate human color perception by including a luminance component and two chromatic components, which represent chromatic information distributed among the four unique hues of human vision: red, green, blue, and yellow[10]. CIELAB has become a standard in various industries and applications because it enables the detection of small color differences, owing to its near-perceptual uniformity. Its device-independence and foundation in human perception make CIELAB a suitable color space for the objective evaluation of color uniformity in mandarins.

E. Statistical analysis

For the specific analysis of red and green shades typical of a tangerine, the a and b channels in the CIELAB color space take on great relevance. The a channel becomes the main component as it captures the variations between red and green, the b channel also contributes to a lesser extent with yellow shades. The luminance channel (L) may not provide relevant information for the analysis of reddish and greenish hues. With a controlled illumination environment, variations in illumination will be minimal. Multivariate statistical analysis in a mandarin *crop* begins by organizing the segmented pixel intensity data into a matrix, where each row corresponds to the intensity values in each pixel of channels a and b , obtaining a column matrix for each channel

$$\mathbf{X} = \begin{bmatrix} a_0 & b_0 \\ a_1 & b_1 \\ \vdots & \vdots \\ a_n & b_n \end{bmatrix} = [\mathbf{a} \quad \mathbf{b}]. \quad (3)$$

The matrix structure of the data allows us to visually represent its channel scatter plot, as shown in Figure 1, the values of channel a stored in $\mathbf{a} = [a_0, a_1, \dots, a_n]^T$ will represent the X-axis, and the values of channel b in $\mathbf{b} = [b_0, b_1, \dots, b_n]^T$ will represent the Y-axis. Each point on the scatter plot corresponds to a pixel of the mandarin orange, and its position is determined by its intensity values in the two channels.

To translate the visual concept of dispersion and clustering into a mathematical basis, the covariance matrix is used, represented in equation 4. The covariance matrix applied to channels \mathbf{a} and \mathbf{b} of the CIELAB space of a mandarin image

$$\mathbf{C}(\mathbf{a}, \mathbf{b}) = \begin{pmatrix} \text{Var}(\mathbf{a}) & \text{Cov}(\mathbf{a}, \mathbf{b}) \\ \text{Cov}(\mathbf{b}, \mathbf{a}) & \text{Var}(\mathbf{b}) \end{pmatrix}, \quad (4)$$

allows us to quantify the joint variability of both data sets based on variance, which measures the dispersion of each channel around its mean, and covariance, which evaluates the linear dependence between channels \mathbf{a} and \mathbf{b} .

Once the covariance matrix has been obtained, the eigenvalues are calculated. In a scatter plot, the eigenvalues indicate the magnitude of the dispersion of the data along the directions where the greatest variability is concentrated; that is, they make it possible to identify in which directions the data are most dispersed, which is essential for assessing the uniformity of the color [11].

F. Index Definition

To define the index, the statistical concepts of covariance matrix and eigenvalues were used. Eigenvalues provide information about the dispersion of the data and are calculated as

$$\det \begin{vmatrix} \text{Var}(\mathbf{a}) - \lambda & \text{Cov}(\mathbf{a}, \mathbf{b}) \\ \text{Cov}(\mathbf{b}, \mathbf{a}) & \text{Var}(\mathbf{b}) - \lambda \end{vmatrix} = 0, \quad (5)$$

where λ represents the eigenvalues obtained by solving the equation.

As a first proposal, the index should be obtained from the product of the eigenvalues, since a higher value would indicate greater dispersion of the data and, therefore, less uniformity. To make the value of the index more intuitive, so that the mandarin with the highest index corresponds to the most uniform mandarin, the index is calculated as

$$\text{IC} = \frac{1}{\pi \cdot e1 \cdot e2}, \quad (6)$$

where $e1$ and $e2$ correspond to the eigenvalues resulting from the covariance matrix.

IV. RESULTS

To validate the performance of the proposed index in the evaluation of color uniformity in mandarins, 30 mandarins detected in the test set were processed. They were subjected to the processing step and subsequently sorted in descending order according to their color uniformity index, representing a quantitative measure inversely proportional to the variation in CIELAB channels a and b . Mandarins in positions 1, 6, 10, 10, 10, 11, 11, 11, 17, 17, 17, 21, 24, and 30 of the resulting ranking are shown in Figure 5. The positions were intentionally chosen to progressively illustrate the change in color uniformity. By visually comparing the eight mandarins, the qualitative and quantitative leap in color distribution reflected in the index values becomes evident, validating its ability to discriminate increasing levels of chromatic incoherence.

Additionally, to test the performance of the index in a controlled manner, a synthetic dataset composed of eight images was designed. Each image represented a “mandarin” as a circle with pure orange chrominance on a completely black background, as shown in Figure 5. To 7 of the 8 images, green pixels randomly distributed within the circle were progressively added, thus simulating increasing levels of chromatic non-uniformity. This approach allowed objective evaluation of the index response to known perturbations.

The results of the synthetic experiment showed a clear inverse correlation, supporting the robustness of the metric to variations in color distribution. Figure 5 illustrates this relationship, showing how the index systematically decreases as the chromatic perturbation increases.

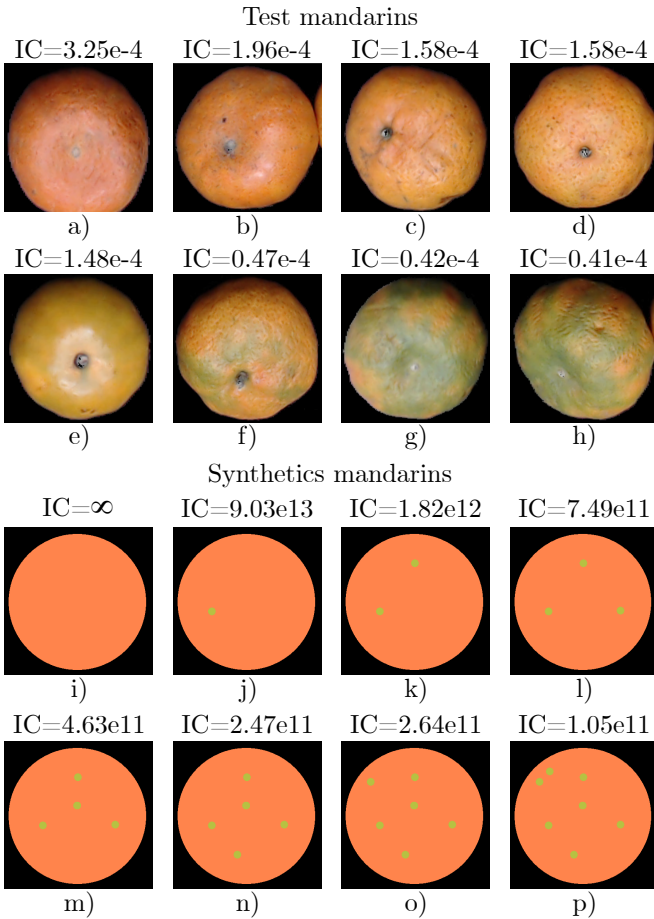


Fig. 5. Organization of mandarin according to its color uniformity index. For the test mandarins a) In 1st place. b) In 6th place. c) In 10th place. d) In 11th place. e) In 17th place. f) In 21st place. g) In 24th place. h) In 30th place. For the synthetic mandarins i) In 1st place. j) In 2nd place. k) In 3rd place. l) In 4th place. m) In 5th place. n) In 6th place. o) In 7th place. p) In 8th place.

V. CONCLUSION

A subsystem was developed to capture images and create a dataset. Through the analysis of technical specifications, a quantitative selection of the camera associated to the subsystem was made. After the camera selection, a Python algorithm was developed to capture and store images. Stored in a dataset, the training and validation images were labeled for subsequent training of the YOLOv11s network. As a final step, a quantitative index was defined to evaluate color uniformity in mandarins. A YOLOv11s algorithm was implemented, selected based on the mAP50-95 metric where a value of 0.98 was obtained. It was trained with the data acquired by the image capture system. An algorithm was also implemented which segmented the YOLO images in order to extract the most important characteristics of the mandarin to define the uniformity index. A quantitative index was defined to calculate color uniformity in mandarins, which is based on the dispersion of the values of channel a and b of the CIELAB color space, identifying patterns of clustering or dispersion and using a covariance matrix to calculate the eigenvalues to establish a quantitative index.

ACKNOWLEDGMENT

This work was supported by ICETEX and MINCIENCIAS through the CTO 2022-0716 Sistema óptico-computacional tipo pushbroom en el rango visible e infrarrojo cercano (VNIR), para la clasificación de frutos cítricos sobre bandas transportadoras mediante aprendizaje profundo, desarrollado en alianza con citricultores de Santander, under Grant 8284.

This work was supported by "Vicerrectoría de Investigación y Extensión - Convocatoria de Apoyo a Docentes de Reciente Vinculación" from Universidad Industrial de Santander, through the project "4276-Sistema optoelectrónico optimizado con inteligencia artificial para tareas de clasificación a través de sensor tipo rolling shutter".

REFERENCES

- [1] Banco Mundial. (2024) Agricultura. [Online]. Available: <https://www.bancomundial.org/es/topic/agriculture/overview>
- [2] Ministerio de Agricultura y Desarrollo Rural, "Cifras sectoriales de cítricos en Colombia," Ministerio de Agricultura y Desarrollo Rural, Tech. Rep., 2021. [Online]. Available: <https://sioc.minagricultura.gov.co/citricos/documentos/2021-03-31%20cifras%20sectoriales.pdf>
- [3] M. Valdes Restrepo, J. Delgado Ospina, L. Londoño-Hernández, and R. A. Rodríguez Restrepo, "Sistema de medición del color como parámetro de calidad en la industria de alimentos," *Temas Agrarios*, vol. 28, no. 1, pp. 69–81, 2023. [Online]. Available: <https://doi.org/10.21897/rta.v28i1.3200>
- [4] K. Mathias-Rettig and K. Ah-Hen, "El color en los alimentos: un criterio de calidad medible," *Agro Sur*, vol. 42, no. 2, pp. 57–66, 2014. [Online]. Available: <https://doi.org/10.4206/agrosur.2014.v42n2-07>
- [5] S. Cubero, F. Albert, D. García Fernández-Pacheco, J. M. Prats-Montalbán, J. Blasco, N. Aleixos *et al.*, "Estimación del índice de color de los cítricos utilizando dispositivos móviles," in *VIII Congreso Ibérico de Agroingeniería*. UMH (Universidad Miguel Hernández), 2016, pp. 926–935.
- [6] C. P. P. Carvalho and J. Londoño Londoño, "Estándares de cosecha y poscosecha para mandarina clementina destinada al mercado en fresco," 2013.
- [7] Higielectronix, "Colorímetro pce instruments pce-csm 1," 2025. [Online]. Available: <https://higielectronix.com/venta-y-mantenimiento-de/equipos-de-medicion-bogota-colombia/colorimetros/pce-instruments-pce-csm-1/>
- [8] M. Miranda, "La imagen digital," *Gen*, vol. 63, no. 2, pp. 134–136, 2009.
- [9] K. Wada, "Labelme: Image polygonal annotation with python," 2021, software disponible bajo licencia GPL-3. [Online]. Available: <https://github.com/wkentaro/labelme>
- [10] Chromatone, "Modelos de color perceptuales," 2025. [Online]. Available: <https://chromatone.center/theory/color/models/perceptual/>
- [11] V. Spruyt, "A geometric interpretation of the covariance matrix," *Computer Vision for Dummies Website*, [https://www.visiondummy.com/2014/04/geometric-interpretation-covariance-matrix/\(accessed 23 June 2021\)](https://www.visiondummy.com/2014/04/geometric-interpretation-covariance-matrix/(accessed 23 June 2021)), 2014.